Onset of η nuclear binding

Nir Barnea[1], *Betzalel* Bazak[1], *Eliahu* Friedman[1], *Avraham* Gal[1,⋆]
Aleš Cieplý[2], *Jiří* Mareš[2], and *Martin* Schäfer[2]

[1] *Racah Institute of Physics, the Hebrew University, Jerusalem 91904, Israel*
[2] *Nuclear Physics Institute, 250 69 Rez, Czech Republic*

Abstract. Recent studies of η nuclear quasibound states by the Jerusalem-Prague Collaboration are reviewed, focusing on stochastic variational method self consistent calculations of η few-nucleon systems. These calculations suggest that a minimum value $\mathrm{Re}\, a_{\eta N} \approx 1$ fm (0.7 fm) is needed to bind $\eta\,^3$He ($\eta\,^4$He).

1 Introduction

The ηN near-threshold interaction is attractive, owing to the $N^*(1535)$ resonance to which the s-wave ηN system is coupled strongly [1]. This has been confirmed in chiral meson-baryon coupled channel models that generate the $N^*(1535)$ dynamically, e.g. [2]. Hence η nuclear quasibound states may exist [3] as also suggested experimentally by the near-threshold strong energy dependence of the $\eta\,^3$He production cross sections shown in Fig. 1. However, the $\eta\,^3$He scattering length deduced in Ref. [4], $a_{\eta\,^3\mathrm{He}} = [-(2.23 \pm 1.29) + i(4.89 \pm 0.57)]$ fm, although of the right sign of its real part, does not satisfy the other necessary condition for a quasibound state pole: $-\mathrm{Re}\, a > \mathrm{Im}\, a$.

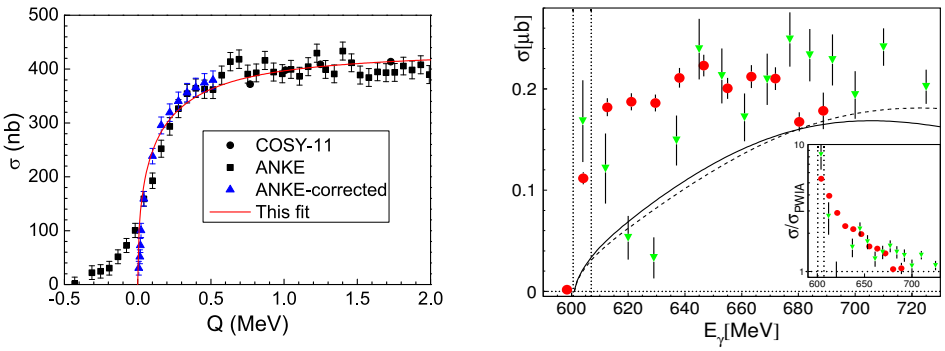

Figure 1. Near-threshold $\eta\,^3$He production cross sections. Left: $dp \to \eta\,^3$He [4]. Right: $\gamma\,^3$He $\to \eta\,^3$He [5].

⋆Presented by A. Gal (avragal@savion.huji.ac.il) at EXA2017, Vienna, Sept. 2017

Quite generally, experimental searches for η nuclear quasibound states in proton, pion or photon induced η production reactions are inconclusive. Regarding the onset of η nuclear binding, Krusche and Wilkin [6] state: "The most straightforward (but not unique) interpretation of the data is that ηd is unbound, $\eta\,^4$He is bound, but that the $\eta\,^3$He case is ambiguous." Indeed, with $\eta\,^3$He almost bound, one might expect that the denser ^{4}He nucleus should help forming a bound $\eta\,^4$He. Nevertheless, a recent Faddeev-Yakubovsky evaluation [7] of the scattering lengths $a_{\eta\,^A\mathrm{He}}$ for both He isotopes, $A = 3, 4$, finds this not to be the case, with the denser ^{4}He apparently leading to a stronger reduction of the subthreshold ηN scattering amplitude than in ^{3}He.

The present overview reports and discusses recent few-body stochastic variational method (SVM) calculations of ηNNN and $\eta NNNN$ using several semi-realistic NN interaction models together with two ηN interaction models that, perhaps, provide sufficient attraction to bind η in the ^{3}He and ^{4}He isotopes [8–10].

2 ηN and NN interaction model input

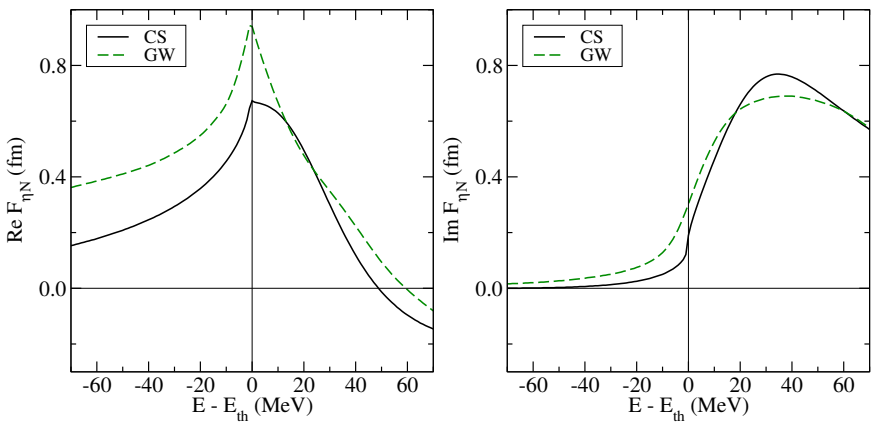

Figure 2. Real and imaginary parts of the ηN cm scattering amplitude near threshold in two meson-baryon coupled channel models: GW [11] and CS [12].

Figure 2 shows ηN s-wave scattering amplitudes $F_{\eta N}(E)$ calculated in two meson-baryon coupled-channel models across the ηN threshold where Re $F_{\eta N}$ has a cusp. These amplitudes exhibit a resonance about 50 MeV above threshold, the $N^*(1535)$. The sign of Re $F_{\eta N}$ below the resonance indicates attraction which is far too weak to bind the ηN two-body system. The threshold values $F_{\eta N}(E_{\rm th})$ are given by the scattering lengths

$$a_{\eta N}^{\rm GW} = (0.96 + i0.26)\ \text{fm}, \quad a_{\eta N}^{\rm CS} = (0.67 + i0.20)\ \text{fm}, \tag{1}$$

with lower values below threshold ($E_{\rm th} = 1487$ MeV). These free-space energy dependent subthreshold amplitudes are transformed to in-medium density dependent amplitudes, in terms of which optical potentials $V_\eta^{\rm opt}(\rho)$ are constructed and used to calculate self consistently η nuclear quasibound states. This procedure was applied in Refs. [13, 14] to several ηN amplitude models, with results for $1s_\eta$ quasibound states in models GW and CS shown in Fig. 3 from ^{12}C to ^{208}Pb.

Figure 3 demonstrates that in both of these ηN amplitude models the $1s_\eta$ binding energy increases with A, saturating in heavy nuclei. Model GW, with larger ηN real and imaginary subthreshold amplitudes than in model CS, gives correspondingly larger values of B_η and Γ_η. While model GW binds

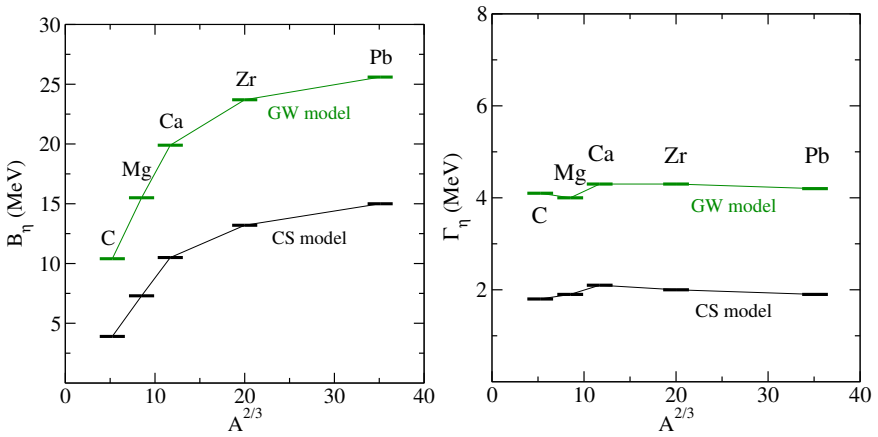

Figure 3. Binding energies B_η (left) and widths Γ_η (right) of $1s_\eta$ quasibound states across the periodic table calculated self consistently [13, 14] using the GW and CS ηN scattering amplitudes of Fig. 2.

η also in nuclei lighter than ^{12}C (not shown in the figure) this needs to be confirmed in few-body calculations.

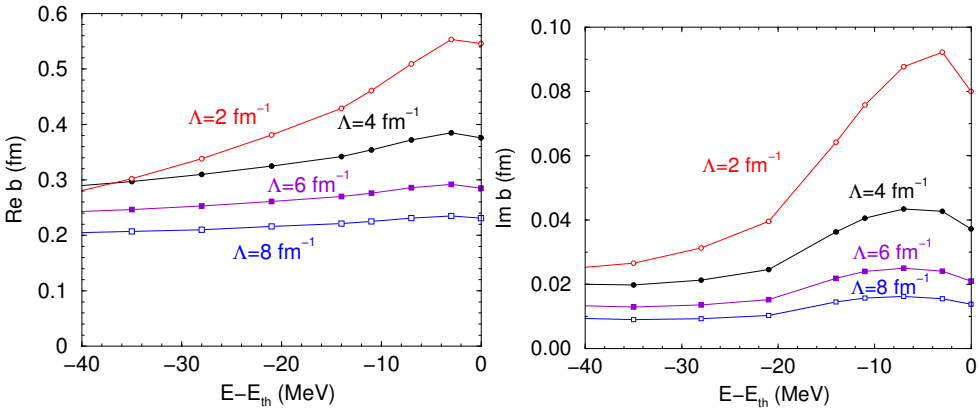

Figure 4. Real and imaginary parts of the strength function $b_\Lambda(E)$ of the effective ηN potential $v^{\rm GW}_{\eta N}(E)$, Eq. (2), obtained from the scattering amplitude $F^{\rm GW}_{\eta N}(E)$ of Fig. 2 below threshold for four values of the scale Λ [9].

Few-body calculations, in distinction from optical model calculations, require the use of effective ηN potentials $v_{\eta N}$ which reproduce the free-space ηN amplitudes below threshold. Fig. 4 shows subthreshold values of the energy dependent strength function $b_\Lambda(E)$ for $v_{\eta N}$ of the form

$$v_{\eta N}(E;r) = -\frac{4\pi}{2\mu_{\eta N}} b_\Lambda(E)\delta_\Lambda(r), \qquad \delta_\Lambda(r) = \left(\frac{\Lambda}{2\sqrt{\pi}}\right)^3 \exp\left(-\frac{\Lambda^2 r^2}{4}\right), \tag{2}$$

derived from the scattering amplitude $F^{\rm GW}_{\eta N}(E)$ of Fig. 2 for several choices of inverse range Λ. The normalized Gaussian function $\delta_\Lambda(r)$ is perceived in $\not\pi$EFT (pionless EFT) as a single ηN zero-range

Dirac $\delta^{(3)}(\mathbf{r})$ contact term (CT), regulated by using a momentum-space scale parameter Λ. Regarding the choice of Λ, substituting the underlying short range vector-meson exchange dynamics by a single regulated CT suggests that the scale Λ is limited to values $\Lambda \lesssim m_\rho$ ($\sim$4 fm^{-1}).

Similarly, a $\not\pi$EFT energy independent $v_{NN}(r)$ is derived at leading order (LO) by fitting a single regulated CT $\sim \delta_\Lambda(r)$ in each spin-isospin s-wave channel to the respective NN scattering length. A pp Coulomb interaction is included. To avoid NNN and ηNN Thomas collapse in the limit $\Lambda \to \infty$, one introduces a three-body regulated CT for each of these three-body systems [9]:

$$V_{NNN}(r_{ij}, r_{jk}) = d^\Lambda_{NNN}\, \delta_\Lambda(r_{ij}, r_{jk}), \qquad V_{\eta NN}(r_{i\eta}, r_{\eta j}) = d^\Lambda_{\eta NN}\, \delta_\Lambda(r_{i\eta}, r_{\eta j}), \tag{3}$$

where $\delta_\Lambda(r_{ij}, r_{jk}) = \delta_\Lambda(r_{ij})\delta_\Lambda(r_{jk})$. The three-nucleon CT d^Λ_{NNN} is fitted to $B_{\rm exp}(^3{\rm He})$. With no further contact terms, $B_{\rm calc}(^4{\rm He})$ is found in this $\not\pi$EFT version [15] to vary moderately with Λ and to exhibit renormalization scale invariance by approaching a finite value $B_{\Lambda\to\infty}(^4{\rm He})$=27.8±0.2 MeV that compares well with $B_{\rm exp}(^4{\rm He})$=28.3 MeV. In contrast, no η-related experimental datum is available for the ηNN CT $d^\Lambda_{\eta NN}$ to be fitted to. Two versions for choosing this CT were tested: (i) $d^\Lambda_{\eta NN} = d^\Lambda_{NNN}$, and (ii) setting $d^\Lambda_{\eta NN}$ so that ηd is just bound, i.e. $B_\eta(\eta d) = 0$. Added to $v^{\rm GW}_{\eta N}(E)$, one finds that each of these versions prevents a potential collapse of ηd, with calculated values of $B(\eta\,^A{\rm He})$ that for $\Lambda \geq 4$ fm^{-1} are nearly independent of the adopted version, as shown in Fig. 7 below.

3 Energy independent $\not\pi$EFT η nuclear few-body calculations

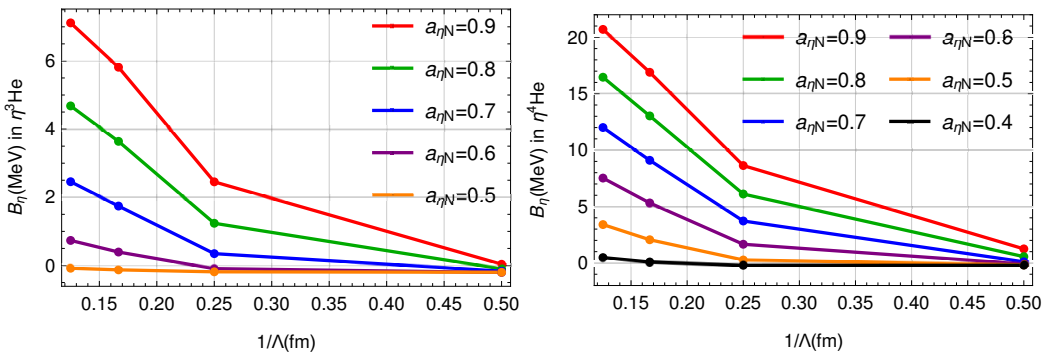

Figure 5. Separation energies B_η obtained in SVM calculations of $\eta\,^3$He (left) and $\eta\,^4$He (right) using $\not\pi$EFT NN and ηN real interactions (2) fitted to values of $a_{\eta N} < 1$ fm, plus a universal NNN and ηNN three-body CT (3), $d^\Lambda_{\eta NN} = d^\Lambda_{NNN}$, as a function of $1/\Lambda$.

Fig. 5 shows η separation energies B_η from $\not\pi$EFT SVM calculations of $\eta\,^3$He and $\eta\,^4$He using energy independent ηN potentials $v_{\eta N}(E{=}E_{\rm th}; r)$ fitted to a given real values of $a_{\eta N}$ for a few values of Λ. The figure suggests that binding $\eta\,^3$He ($\eta\,^4$He) requires that $a_{\eta N} \geq 0.55$ fm (0.45 fm), compatible with an effective value ${\rm Re}\, a'_{\eta N}$=0.48±0.05 fm derived for a nearly bound $\eta\,^3$He [4]. For input values of $a_{\eta N}$ higher than shown in the figure, beginning at $a_{\eta N}{\approx}1.2$ fm, the calculated binding energies $B^{A=3,4}_\eta(\Lambda > 4\ {\rm fm}^{-1})$ diverge, apparently since ηd becomes bound then at Λ=4 fm^{-1} [8]. Qualitative arguments in support of this ηd onset-of-binding value of $a_{\eta N}$ are given here in Appendix A.

4 Energy dependence in η nuclear few-body systems

Having derived energy dependent ηN potentials $v_{\eta N}(E;r)$, see Eq. (2) and Fig. 4, a two-body subthreshold input energy $\delta\sqrt{s} \equiv E - E_{\rm th}$ needs to be chosen. However, $\delta\sqrt{s}$ is not conserved in the η nuclear few-body problem, so the best one can do is to require that this choice agrees with the expectation value $\langle\,\delta\sqrt{s}\,\rangle$ generated in solving the few-body problem, as given by [10]

$$\langle\delta\sqrt{s}\rangle = -\frac{B}{A} - \xi_N\frac{1}{A}\langle T_A\rangle + \frac{A-1}{A}\mathcal{E}_\eta - \xi_A\xi_\eta\left(\frac{A-1}{A}\right)^2\langle T_\eta\rangle. \tag{4}$$

Here $\xi_{N(\eta)} = m_{N(\eta)}/(m_N + m_\eta)$, $\xi_A = Am_N/(Am_N + m_\eta)$, T_A and T_η denote the nuclear and η kinetic energy operators in appropriate Jacobi coordinates, B is the total binding energy, and $\mathcal{E}_\eta = \langle H - H_N\rangle$ with each Hamiltonian defined in its own cm frame. Self consistency (SC), $\langle\,\delta\sqrt{s}\,\rangle = \delta\sqrt{s}$, is imposed in our calculations, as demonstrated graphically in Fig. 6 (left). Applications of SC to meson-nuclear systems are reviewed in Ref. [16]. For recent K^--atom and nuclear applications see Refs. [17, 18]. More recently, Hoshino et al. [19] argued in a K^-d study that by applying this procedure one violates the requirement of total momentum conservation. In Appendix B here we show specifically for $A = 2$ that our choice of SC Eq. (4) is not in conflict with any conservation law.

Finally, we note that Eq. (4) in the limit $A >> 1$ coincides with the optical model downward energy shift (supplemented by a Coulomb term) used in recent K^- atom and nuclear studies [17, 18]:

$$\langle\delta\sqrt{s}\rangle = -B_N\frac{\rho}{\bar\rho} - \xi_N B_\eta\frac{\rho}{\rho_0} - \xi_N T_N\left(\frac{\rho}{\bar\rho}\right)^{2/3} + \xi_\eta \mathrm{Re}\,V_\eta^{\rm opt}(\delta\sqrt{s}), \tag{5}$$

where $T_N = \langle T_A\rangle/A = 23.0$ MeV at the average nuclear density $\bar\rho$, $B_N = B_{\rm nuc}/A \approx 8.5$ MeV is an average nucleon binding energy and B_η denotes the calculated η separation energy. All terms here are negative, thereby leading to a downward energy shift.

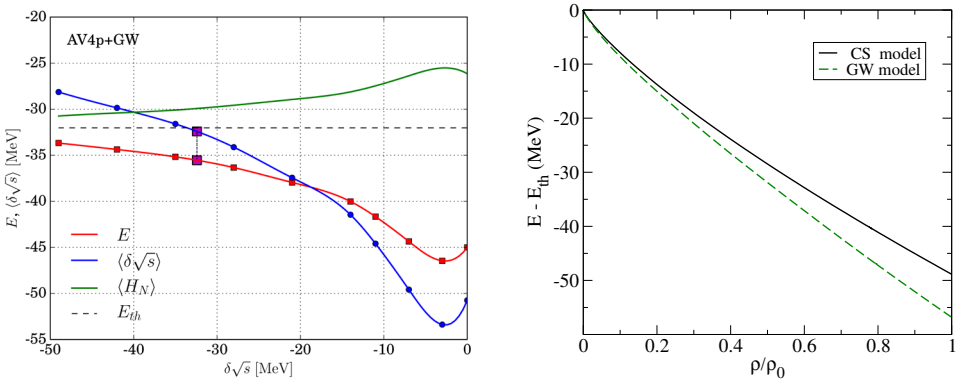

Figure 6. Left: $\eta\,^4$He bound state energy E (red, squares) and the expectation value $\langle\delta\sqrt{s}\rangle$ (blue, circles), calculated using the AV4' NN potential (denoted here AV4p), as a function of the input energy argument $\delta\sqrt{s}$ of the GW ηN potential with $\Lambda = 4$ fm^{-1}. The dotted vertical line marks the self consistent output values of $\langle\delta\sqrt{s}\rangle$ and E. The horizontal dashed line denotes the calculated ^{4}He g.s. energy, marking the threshold of η binding. The green curve shows the expectation value $< H_N >$ of the nuclear core energy. Right: subthreshold ηN energies $\delta\sqrt{s} = E - E_{\rm th}$ probed by the η nuclear optical potential as a function of the relative nuclear RMF density in Ca. Each of the two curves was calculated self consistently for a particular ηN subthreshold amplitude model.

The SC procedure is demonstrated in Fig. 6 (left) for $\eta\,^4$He binding energy calculated using the AV4' *NN* potential and GW ηN potential with Λ=4 fm^{-1}. The $\eta\,^4$He bound state energy E (excluding rest masses) and the output expectation value $\langle\delta\sqrt{s}\rangle$, where $\delta\sqrt{s}$ stands for the ηN cm energy with respect to its threshold value $E_{\rm th}$, are plotted as a function of the subthreshold input energy argument $\delta\sqrt{s}$ of the potential $v^{\rm GW}_{\eta N}$. The SC condition requires $\delta\sqrt{s} = \langle\delta\sqrt{s}\rangle$ which is satisfied at -32.4 MeV. The corresponding value of $E(\langle\delta\sqrt{s}\rangle)$ then represents the SC energy of $\eta\,^4$He, with $B^{\rm SC}_\eta = 3.5$ MeV, considerably less than the value $B^{\rm th}_\eta = 13$ MeV obtained by disregarding the energy dependence of $v^{\rm GW}_{\eta N}$ and using its threshold value corresponding to $\delta\sqrt{s} = 0$.

In Fig. 6 (right) we present the ηN downward energy shift $\delta\sqrt{s} = E - E_{\rm th}$ as a function of the relative nuclear density ρ/ρ_0 in Ca, evaluated self consistently via Eq. (5) in the CS and GW models. The energy shift at ρ_0 is -55 ± 10 MeV, about twice larger than the SC condition $\delta\sqrt{s} = -B_\eta$ applied in some other works, e.g. [20]. The GW shift exceeds the CS shift owing to the stronger GW amplitude of Fig. 2 and both were incorporated in the calculation of $1s_\eta$ quasibound nuclear states, Fig. 3.

5 Results of η nuclear few-body calculations

Our fully self consistent ηNN, ηNNN and $\eta NNNN$ bound-state calculations [8–10] use the following nuclear core models: (i) $\not\pi$EFT including a three-body contact term [15], (ii) AV4p, a Gaussian basis adaptation of the Argonne AV4' *NN* potential [21], and (iii) MNC, the Minnesota soft core *NN* potential [22]. Models GW [11] and CS [12] were used to generate energy dependent ηN potentials which prove too weak to bind any ηNN system when using AV4p or MNC for the nuclear core model. Calculated η separation energies B_η are shown in Figs. 7 and 8.

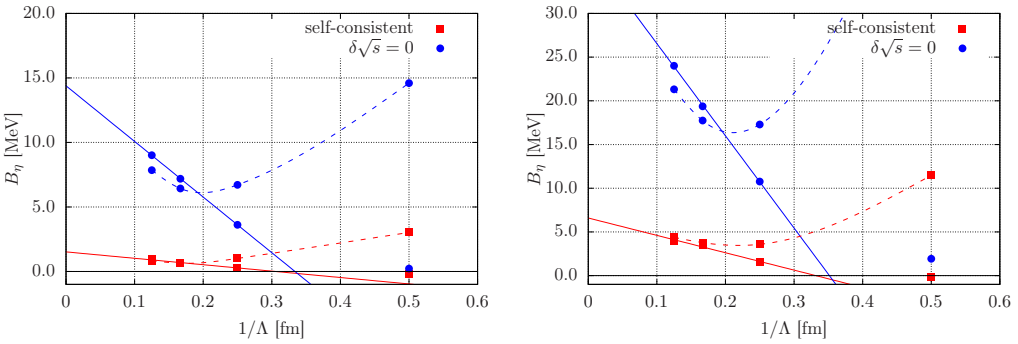

Figure 7. $B_\eta(\eta\,^3$He) (left) and $B_\eta(\eta\,^4$He) (right) as a function of $1/\Lambda$ from $\not\pi$EFT few-body calculations [9] using $v^{\rm GW}_{\eta N}$, with (squares) & without (circles) imposing self consistency. Solid lines: $d^\Lambda_{\eta NN} = d^\Lambda_{NNN}$, dashed lines: $d^\Lambda_{\eta NN}$ ensuring that $B_\eta(\eta d) = 0$.

Fig. 7 demonstrates in $\not\pi$EFT the moderating effect that imposing SC (red, squares) by using $v^{\rm GW}_{\eta N}(E_{\rm sc})$, rather than using threshold values $v^{\rm GW}_{\eta N}(E_{\rm th})$ (blue, circles), bears on the calculated B_η values and their Λ scale dependence [9]. Near Λ=4 fm^{-1}, imposing sc lowers $B_\eta(\eta\,^3$He) by close to 5 MeV and $B_\eta(\eta\,^4$He) by close to 10 MeV. The figure demonstrates that $B_\eta(\eta\,^4$He) is always larger than $B_\eta(\eta\,^3$He). Focusing on scale parameters near Λ=4 fm^{-1} one observes that $\eta\,^3$He is hardly bound by a fraction of MeV, whereas $\eta\,^4$He is bound by a few MeV. The choice of three-body CT $d^\Lambda_{\eta NN}$ hardly matters for $\Lambda > 4$ fm^{-1}, becoming substantial at $\Lambda < 4$ fm^{-1}.

Fig. 8 demonstrates in non-EFT calculations the dependence of B_η, calculated self consistently, on the choice of NN and ηN interaction models. Using the more realistic AV4' NN interaction results in less η binding than using the soft-core MNC NN interaction. For $v_{\eta N}^{\rm GW}$ near Λ=4 fm^{-1} the difference amounts to about 0.3 MeV for $\eta\,^3$He and about 1.5 MeV for $\eta\,^4$He; $\eta\,^3$He appears then barely bound whereas $\eta\,^4$He is bound by a few MeV. The weaker $v_{\eta N}^{\rm CS}$ does not bind $\eta\,^3$He and barely binds $\eta\,^4$He using the MNC NN interaction, implying that $\eta\,^4$He is unlikely to bind for the more realistic AV4' NN interaction. For smaller, but still physically acceptable values of Λ down to $\Lambda = 2$ fm^{-1}, $\eta\,^3$He becomes unbound and $\eta\,^4$He is barely bound using the AV4' NN and GW ηN interactions.

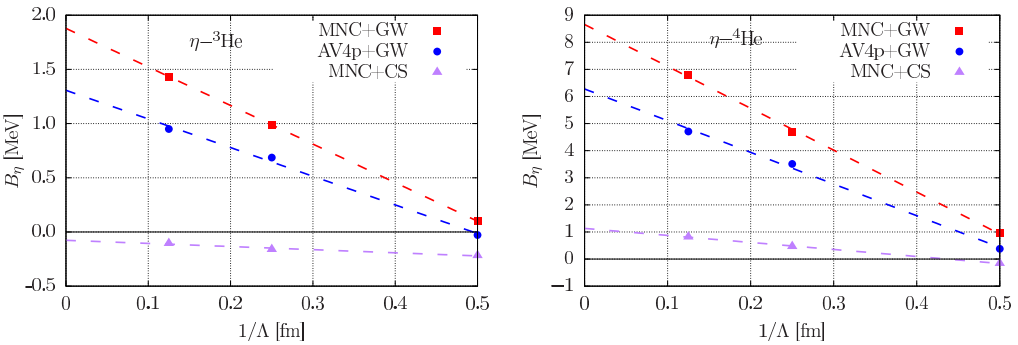

Figure 8. $B_\eta(\eta\,^3\mathrm{He})$ (left) and $B_\eta(\eta\,^4\mathrm{He})$ (right) as a function of $1/\Lambda$ from few-body calculations [10] using NN and ηN interactions, as marked, and imposing self consistency.

The B_η values calculated in Refs. [8–10] were calculated assuming real Hamiltonians, justified by Im $v_{\eta N} \ll$ Re $v_{\eta N}$ from Fig. 4. This approximation is estimated to add near threshold less than 0.3 MeV to B_η. Perturbatively-calculated widths Γ_η of weakly bound states amount to only few MeV, outdating those reported in Ref. [8].

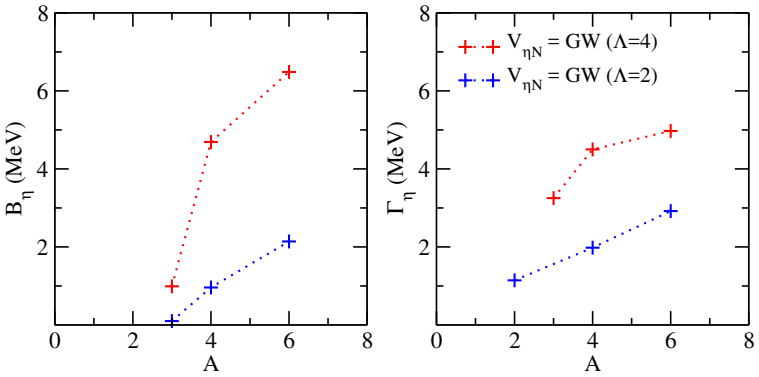

Figure 9. Preliminary SVM results for binding energies B_η (left) and widths Γ_η (right) of $1s_\eta$ quasibound states in ^{3}He, ^{4}He and ^{6}Li, calcualted using the Minnesota NN potential and the GW ηN potential for $\Lambda = 2$ and 4 fm^{-1}.

In future work it will be interesting to extend the present SVM few-body calculations to heavier nuclei, beginning with light p-shell nuclei. This represents highly non-trivial task. In Fig. 9 we

present preliminary results for $\eta\,^6$Li, using the central Minnesota NN and GW ηN potentials. In this calculation the ^{6}Li nuclear core consisted of a single $S = 1, T = 0$ spin-isospin configuration, yielding $B(^6\mathrm{Li})$=34.66 MeV which is short by almost 2 MeV with respect to a calculation reported in Ref. [24] that used the same NN interaction while including more spin-isospin configurations. The figure suggests that $\eta\,^6$Li is comfortably bound, even for as low value of scale parameter as $\Lambda = 2$ fm^{-1}.

6 Summary

Based mostly on the AV4' results in Fig. 8, which are close to the $\not\pi$EFT results in Fig. 7, we conclude that $\eta\,^3$He becomes bound for $\mathrm{Re}\,a_{\eta N} \sim 1$ fm, as in model GW, while $\eta\,^4$He binding requires a lower value of $\mathrm{Re}\,a_{\eta N} \sim 0.7$ fm, almost reached in model CS. These $\mathrm{Re}\,a_{\eta N}$ onset values, obtained by incorporating the requirements of ηN subthreshold kinematics, are obviously *larger* than those estimated in Sect. 3 upon calculating with $v_{\eta N}(E = E_{\rm th}; r)$ threshold input. Finally, $\mathrm{Re}\,a_{\eta N} < 0.7$ fm if $\eta\,^4$He is unbound, as might be deduced from the recent WASA-at-COSY search [23].

Appendix A: Onset of ηd binding

Here we apply the Brueckner formula [25], expressing the ηd scattering length in terms of the ηN scattering length, to discuss qualitatively the onset of ηd binding. This formula was originally proposed for a system of a light meson (π meson) and two heavy static nucleons. More recently it was used to estimate the $K^- d$ scattering length (see derivation and discussion in Ref. [26]) where the meson-nucleon mass ratio is similar to that for ηN. For ηd the Brueckner formula assumes the form

$$a_{\eta d} = \int a_{\eta d}(r)|\psi_d(\mathbf{r})|^2 \mathrm{d}\mathbf{r}\,, \tag{6}$$

$$a_{\eta d}(r) = \left(1 + \frac{m_\eta}{m_d}\right)^{-1} \frac{\tilde{a}_p + \tilde{a}_n + 2\tilde{a}_p\tilde{a}_n/r}{1 - \tilde{a}_p\tilde{a}_n/r^2}\,, \tag{7}$$

where $\tilde{a} = (1 + m_\eta/m_N)a$, with a_p and a_n standing for $a_{\eta p}$ and $a_{\eta n}$ respectively in the ηN cm system. The numerator in the Brueckner formula consists of single- and double-scattering terms, whereas the denominator provides for the renormalization of these terms by higher-order scattering terms. Since $a_p = a_n$ for the isoscalar η meson, Eq. (7) reduces to a simpler form,

$$a_{\eta d}(r) = \frac{2}{1 + \frac{m_\eta}{m_d}} \frac{\tilde{a}_{\eta N}}{1 - \tilde{a}_{\eta N}/r}\,, \tag{8}$$

which leads to the following approximate expression:

$$a_{\eta d} = \frac{2}{1 + \frac{m_\eta}{m_d}} \frac{\tilde{a}_{\eta N}}{1 - \tilde{a}_{\eta N}\langle 1/r\rangle_d}\,, \tag{9}$$

with expansion parameter $\tilde{a}\,\langle 1/r\rangle_d$, where $\langle 1/r\rangle_d \approx 0.45$ fm^{-1} for a realistic deuteron wavefunction [27]. Hence, this multiple scattering series faces divergence for sufficiently large ηN scattering length, say $a > 1.4$ fm.

Several straightforward applications of Eq. (9) are as follows:

- For $\mathrm{Re}\, a_{\eta N}^{\mathrm{GW}} = 0.96$ fm, suppressing $\mathrm{Im}\, a_{\eta N}^{\mathrm{GW}}$, one gets $a_{\eta d} = 7.46$ fm. Increasing this GW input value of $a_{\eta N}$, a critical value $a_{\eta N}^{\mathrm{crit}} = 1.40$ fm is reached at which the denominator in Eq. (9) vanishes, signaling the appearance of a zero-energy ηd bound state.
- The LO $\not\pi$EFT nuclear calculations [15] yield a more compact deuteron, $r_{\mathrm{rms}} = 1.55$ fm for $\Lambda \to \infty$ compared to the 'experimental' value $r_{\mathrm{rms}} = 1.97$ fm. Scaling the value $\langle 1/r \rangle_d = 0.45$ used in Eq. (9) by 1.97/1.55, one gets $a_{\eta d} = 18.1$ fm and $a_{\eta N}^{\mathrm{crit}} = 1.10$ fm.
- For the fully complex scattering length $a_{\eta N}^{\mathrm{GW}} = 0.96 + i0.26$ fm, one gets $a_{\eta d} = 4.66 + i4.76$ fm. Increasing $\mathrm{Re}\, a_{\eta N}$ at a frozen value of $\mathrm{Im}\, a_{\eta N}$, $\mathrm{Re}\, a_{\eta d}$ reverses its sign at $\mathrm{Re}\, a_{\eta N}^{\mathrm{crit}} = 1.35$ fm while $\mathrm{Im}\, a_{\eta d}$ keeps positive all through.
- At $\mathrm{Re}\, a_{\eta N}^{\mathrm{crit}} = 1.59$ fm, $|\mathrm{Re}\, a_{\eta d}|$ becomes larger than $\mathrm{Im}\, a_{\eta d}$, which signals a threshold ηd bound state.

Appendix B: ηN subthreshold kinematics

Here we outline the choice of the ηN subthreshold energy shift $\delta\sqrt{s} \equiv \sqrt{s_{\eta N}} - (m_N + m_\eta)$ applied in our η nuclear few-body works [8–10], see Eq. (4), with emphasis on the three-body ηd system. Since the ηN effective potential $v_{\eta N}$ discussed in Sect. 2 is energy dependent, one needs to determine as consistently as possible a fixed *input* value $\delta\sqrt{s}$ at which $v_{\eta N}$ should enter the η nuclear few-body calculation. The two-body Mandelstam variable $\sqrt{s_{\eta N}} = \sqrt{(E_\eta + E_N)^2 - (\vec{p}_\eta + \vec{p}_N)^2}$ which reduces to $(E_\eta + E_N)$ in the ηN two-body cm system is not a conserved quantity in the η nuclear few-body problem since spectator nucleons move the interacting ηN two-body subsystem outside of its cm system. We proceed to evaluate the expectation value of *output* values of $\delta\sqrt{s}$, replacing $\sqrt{s_{\eta N}}$ by $(1/A)\sum_{i=1}^{A} \sqrt{(E_\eta + E_i)^2 - (\vec{p}_\eta + \vec{p}_i)^2}$ due to the antisymmetry of the nuclear wavefunction. Expanding about the ηN threshold, one gets in leading order of p^2

$$\langle\, \delta\sqrt{s}\,\rangle \approx \frac{1}{A}\,\langle \sum_{i=1}^{A}(\mathcal{E}_\eta + \mathcal{E}_i) - \sum_{i=1}^{A}\frac{(\vec{p}_\eta + \vec{p}_i)^2}{2(m_N + m_\eta)}\,\rangle, \tag{10}$$

where $\mathcal{E}_\eta = E_\eta - m_\eta$ and $\mathcal{E}_i = E_i - m_N$. Since $\sum_{i=1}^{A}\mathcal{E}_i$ is naturally identified with the expectation value of the nuclear Hamiltonian H_N, $\sum_{i=1}^{A}\mathcal{E}_i = \langle H_N\rangle = E_{\mathrm{nuc}} = -B_{\mathrm{nuc}}$, it is natural and also consistent to identify $\mathcal{E}_\eta$ with the expectation value of $(H - H_N)$, $\mathcal{E}_\eta = \langle H - H_N\rangle$. Furthermore, recalling that $\mathcal{E}_\eta + \sum_{i=1}^{A}\mathcal{E}_i = E = -B$, where $E = \langle H\rangle$ is the total η nuclear energy and B is the total binding energy, the sum over the momentum independent part in Eq. (10) gives $[-B + (A-1)\mathcal{E}_\eta]/A$, thereby reproducing two of the four terms in Eq. (4). Note that $\mathcal{E}_\eta$ is negative and its magnitude exceeds the η separation energy B_η. The sum over the momentum dependent part of Eq. (10) yields the other two terms of Eq. (4), which we demonstrate for ηd, $A = 2$.

Since the ηd calculation employes translationally invariant coordinate sets, the total momentum vanishes sharply: $(\vec{p}_\eta + \vec{p}_1 + \vec{p}_2) = 0$. We then substitute $\vec{p}_1^{\,2}$ for $(\vec{p}_\eta + \vec{p}_2)^2$ and $\vec{p}_2^{\,2}$ for $(\vec{p}_\eta + \vec{p}_1)^2$ in the momentum dependent part in Eq. (10), resulting in momentum dependence proportional to $\vec{p}_1^{\,2} + \vec{p}_2^{\,2}$. This is rewritten as

$$\vec{p}_1^{\,2} + \vec{p}_2^{\,2} = \frac{1}{2}[(\vec{p}_1 - \vec{p}_2)^2 + (\vec{p}_1 + \vec{p}_2)^2] = 2\vec{p}_{N:N}^{\,2} + \frac{1}{2}\vec{p}_\eta^{\,2}, \tag{11}$$

where $\vec{p}_{N:N}$ is the nucleon-nucleon relative momentum operator. To obtain the η momentum operator $\vec{p}_\eta$ on the r.h.s. we used again total momentum conservation. Finally, transforming $\vec{p}_{N:N}^{\,2}$ and $\vec{p}_\eta^{\,2}$ to

intrinsic kinetic energies, $T_{N:N}$ for the internal motion of the deuteron core and T_η for that of the η meson with respect to the NN cm, one gets for this $A = 2$ special case

$$\langle \delta \sqrt{s} \rangle_{\eta d} \approx -\frac{1}{2}\left(B - \mathcal{E}_\eta + \xi_N \langle T_{N:N} \rangle + \xi_{A=2}\xi_\eta \frac{1}{2}\langle T_\eta \rangle\right), \tag{12}$$

which agrees with Eq. (4) for $A = 2$ upon realizing that $T_{N:N}$ here coincides with $T_{A=2}$ there. To get idea of the relative importance of the various terms in this expression, we assume a near-threshold ηd bound state for which both $\mathcal{E}_\eta$ and $\langle T_\eta \rangle$ are negligible (fraction of MeV each) and $B \to B_d \approx 2.2$ MeV. With $\langle T_{N:N} \rangle \to \langle T_d \rangle$, and with a deuteron kinetic energy $\langle T_d \rangle$ in the range of 10 to 20 MeV, this term provides the largest contribution to the downward energy shift which is then of order −5 MeV for the diffuse deuteron nuclear core.

Acknowledgments

The work of A.C., J.M. and M.S. was supported by the GACR Grant No. P203/15/04301S.

References

[1] R.S. Bhalerao, L.C. Liu, Phys. Rev. Lett. **54**, 865 (1985)
[2] N. Kaiser, P.B. Siegel, W. Weise, Phys. Lett. B **362**, 23 (1995)
[3] Q. Haider, L.C. Liu, Phys. Lett. B **172**, 257 (1986)
[4] J.J. Xie, W.H. Liang, E. Oset, P. Moskal, M. Skurzok, C. Wilkin, Phys. Rev. C **95**, 015202 (2017)
[5] F. Pheron et al., Phys. Lett. B **709**, 21 (2012)
[6] B. Krusche, C. Wilkin, Prog. Part. Nucl. Phys. **80**, 43 (2015)
[7] A. Fix, O. Kolesnikov, Phys. Lett. B **772**, 663 (2017)
[8] N. Barnea, E. Friedman, A. Gal, Phys. Lett. B **747**, 345 (2015)
[9] N. Barnea, B. Bazak, E. Friedman, A. Gal, Phys. Lett. B **771**, 297 (2017), **775**, 364 (2017)
[10] N. Barnea, E. Friedman, A. Gal, Nucl. Phys. A **968**, 35 (2017)
[11] A.M. Green, S. Wycech, Phys. Rev. C **71**, 014001 (2005)
[12] A. Cieplý, J. Smejkal, Nucl. Phys. A **919**, 46 (2013)
[13] E. Friedman, A. Gal, J. Mareš, Phys. Lett. B **725** 334 (2013)
[14] A. Cieplý, E. Friedman, A. Gal, J. Mareš, Nucl. Phys. A **925**, 126 (2014)
[15] J. Kirscher, E. Pazy, J. Drachman, N. Barnea, Phys. Rev. C **96**, 024001 (2017)
[16] A. Gal, E. Friedman, N. Barnea, A. Cieplý, J. Mareš, D. Gazda, Acta Phys. Polon. B **45**, 673 (2014)
[17] E. Friedman, A. Gal, Nucl. Phys. A **959**, 66 (2017)
[18] J. Hrtánková, J. Mareš, Phys. Lett. B **770**, 342 (2017), Phys. Rev. C **96**, 015205 (2017)
[19] T. Hoshino, S. Ohnishi, W. Horiuchi, T. Hyodo, W. Weise, Phys. Rev. C **96**, 045204 (2017)
[20] C. García-Recio, T. Inoue, J. Nieves, E. Oset, Phys. Lett. B **550**, 47 (2002)
[21] R.B. Wiringa, S.C. Pieper, Phys. Rev. Lett. **89**, 182501 (2002)
[22] D.R. Thompson, M. LeMere, Y.C. Tang, Nucl. Phys. A **286**, 53 (1977)
[23] P. Adlarson, et al. (WASA-at-COSY Collab.), Nucl. Phys. A **959**, 102 (2017)
[24] P. Navrátil, E. Caurier, Phys. Rev. C **69**, 014311 (2004)
[25] K.A. Brueckner, Phys. Rev. **89**, 834 (1953)
[26] A. Gal, Int. J. Mod. Phys. A **22**, 226 (2007)
[27] M. Pavón Valderrama, E. Ruiz Arriola, arXiv:nucl-th/0605078